Singlet Photochemistry in Model Photosynthesis: Identification of Charge Separated Intermediates by Fourier Transform and CW-EPR Spectroscopies

Kobi Hasharoni,[1a,b] Haim Levanon,*[1a,b] Jau Tang,[1a] Michael K. Bowman,[1a] James R. Norris,[1a] Devens Gust,[1c] Thomas A. Moore,[1c] and Ana L. Moore[1c]

Contribution from the Chemistry Division, Argonne National Laboratory, Argonne, Illinois 60439, Department of Physical Chemistry and The Fritz Haber Research Center for Molecular Dynamics, The Hebrew University of Jerusalem, Jerusalem 91904, Israel, and Department of Chemistry, Arizona State University, Tempe, Arizona 85287.
Received January 25, 1990

Abstract: Intramolecular electron transfer from the photoexcited state of a carotenoid–porphyrin–diquinone tetrad was studied by selective laser excitation with both Fourier transform and CW EPR spectroscopies. It is shown that the electron transfer occurs from the singlet state of the porphyrin constituent to produce the terminal benzoquinone radical anion and the carotenoid radical cation. This tetrad molecule can maintain the charge-separated state for a substantial period of time (~1 μs), allowing the characterization of the short-lived radicals. The derivative-like spectrum of the quinone radical anion and its dependence on the turning angle of the microwave pulse indicates that electron transfer proceeds via the singlet state.

Introduction

Primary photoinduced charge separation is initiated in bacterial and, most probably, in green plant photosynthesis, via the singlet radical-pair (RP) state. The initial electron transfer occurs on the picosecond time scale,[2,3] while subsequent electron transfers occur on a time range from hundreds of picoseconds to microseconds. Although time-resolved optical spectroscopic methods have traditionally been used to study these events, the new magnetic resonance technique of Fourier transform electron paramagnetic resonance (FT-EPR) is well-suited for characterizing the spin state and spin dynamics of these new charge-separated species.[4-10]

Simple model photosynthetic systems have failed to mimic the natural one in that either the electron transfer occurs from triplet-state precursor, or the charge recombination reactions are too fast to allow detection of the charge-separated states by EPR spectroscopy. The recent development of multicomponent molecular species demonstrating multistep electron transfer has made possible the generation of long-lived (hundreds of nanoseconds to microseconds) charge-separated states with high quantum yields.[11] This new generation of photosynthesis mimics is ideally suited to study by the new EPR techniques. Here, we characterize the photoinduced, charge-separated state in a carotenoid–porphyrin–diquinone tetrad[11-13] (**1**) using laser excitation combined with FT-EPR and diode detection CW-EPR spectroscopies. FT-EPR has for the first time allowed detection and identification of both radical ions in the $C^{\bullet+}$–P–Q_A–$Q_B^{\bullet-}$ charge-separated state (carotenoid radical cation and quinone radical anion). In addition, the lifetime of the state and its singlet state genesis have been confirmed.

Scheme I

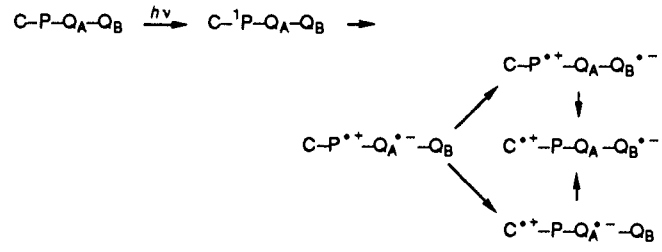

Time-resolved optical studies of **1** and related compounds suggested that the optical excitation of the porphyrin moiety produces a series of electron-transfer steps depicted in Scheme I. An electron is transferred from the lowest excited singlet state of the porphyrin to the adjacent naphthoquinone moiety with a rate of 6.7×10^{10} s^{-1} to produce a radical ion pair C–$P^{\bullet+}$–$Q_A^{\bullet-}$–Q_B. This initial state ultimately is thought to produce $C^{\bullet+}$–P–Q_A–$Q_B^{\bullet-}$ as inferred from the characteristic optical absorption of the carotenoid radical cation moiety. The quinone anion was not detected optically and no direct evidence of the spin multiplicity was obtained. This final species is formed with a quantum yield of 0.23 at 295 K and 0.5 at 240 K in dichloromethane, with lifetimes of 460 and 2800 ns, respectively.[11-13]

Experimental Section

The synthesis of the tetrad, **1**, is described elsewhere.[13] FT-EPR measurements (for experimental details see ref 6, 7, 9, and 10) were performed on samples of **1** in dichloromethane (~4 μM) in 4-mm o.d. Suprasil EPR tubes. Samples were degassed by several freeze–pump–thaw cycles on a vacuum line. Sample temperature (240 K) was maintained using a nitrogen variable-temperature flow dewar in the EPR resonator. Samples were excited at 591 nm (1 mJ/pulse at 100 Hz) from an excimer-pumped dye laser (Lambda Physik EMG-50E using XeCl) which corresponds to the Q-band absorption of the porphyrin. The pulsed EPR experiments were carried out by using one or two microwave pulses synchronized to the laser pulses. The free induction decay (FID) was recorded in the one-pulse experiment while the shape of the spin–echo was recorded in the two-pulse experiments. The turning angle of the microwave pulses and spectral phases were calibrated by using a stable solution of the duroquinone radical anion as a standard, while keeping the spectrometer setup unchanged for all samples. The standard was prepared by partial photolysis of a sealed deoxygenated solution of 10 mM duroquinone in a 2-propanol/KOH solution containing triethylamine as an electron donor. Photolysis was carried out with the 308-nm output of an excimer laser to approximately 1 mM in radical concentration. The

(1) (a) Argonne National Laboratory. (b) Hebrew University of Jerusalem. (c) Arizona State University.
(2) For a comprehensive treatment of in vivo and model photosynthesis, see, e.g.: *Isr. J. Chem.* **1988**, 28.
(3) Friesner, R. A.; Youngdo, W. *Biochem. Biophys. Acta*, in press.
(4) For a review on fast EPR detection in liquids, see, e.g.: Trifunac, A. D.; Lawler, R. G.; Bartels, D. M.; Thurnauer, M. C. *Prog. Reaction Kinet.* **1986**, *14*, 43.
(5) Depew, M. C.; Wan, K. S. *J. Phys. Chem.* **1986**, *90*, 6597.
(6) Massoth, R. J. Ph.D. Thesis, University of Kansas, 1987.
(7) Angerhofer, A.; Massoth, R. J.; Bowman, M. K. *Isr. J. Chem.* **1988**, *28*, 227.
(8) Prisner, T.; Dobbert, O.; Dinse, K. P.; van Willigen, H. *J. Am. Chem. Soc.* **1988**, *110*, 1622.
(9) Angerhofer, A.; Toporowicz, M.; Bowman, M. K.; Norris, J. R.; Levanon, H. *J. Phys. Chem.* **1988**, *92*, 71.
(10) Bowman, M. K.; Toporowicz, M.; Norris, J. R.; Michalski, T. J.; Angerhofer, A.; Levanon, H. *Isr. J. Chem.* **1988**, *28*, 215 and references therein.
(11) Gust, D.; Moore, T. A. *Science* **1989**, *244*, 35.
(12) Gust, D.; Moore, T. A.; Moore, A. L.; Barrett, D.; Harding, L. O.; Makings, L. R.; Liddell, P. A.; De Schryver, F. C.; Van der Auweraer, M.; Benasson, R. V.; Rougee, M. *J. Am. Chem. Soc.* **1988**, *110*, 321.
(13) Gust, D.; Moore, T. A.; Moore, A. L.; Seely, G.; Liddell, P. A.; Barrett, D.; Harding, L. O.; Ma, X. C.; Lee, S. J.; Gao, F. *Tetrahedron*, in press.

0002-7863/90/1512-6477$02.50/0

Chart I

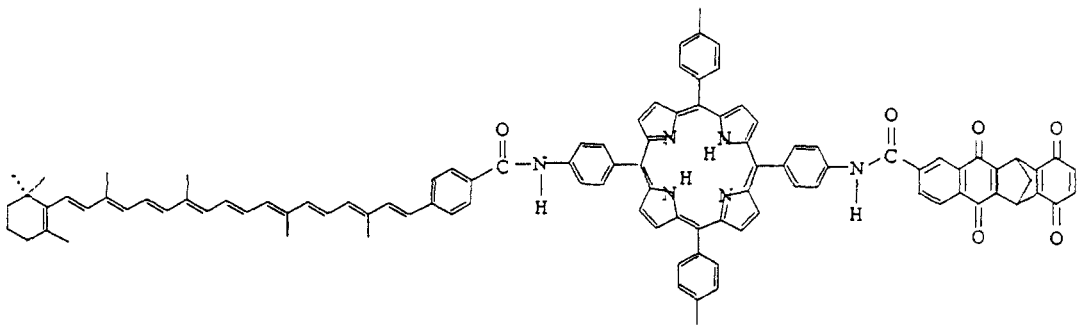

1

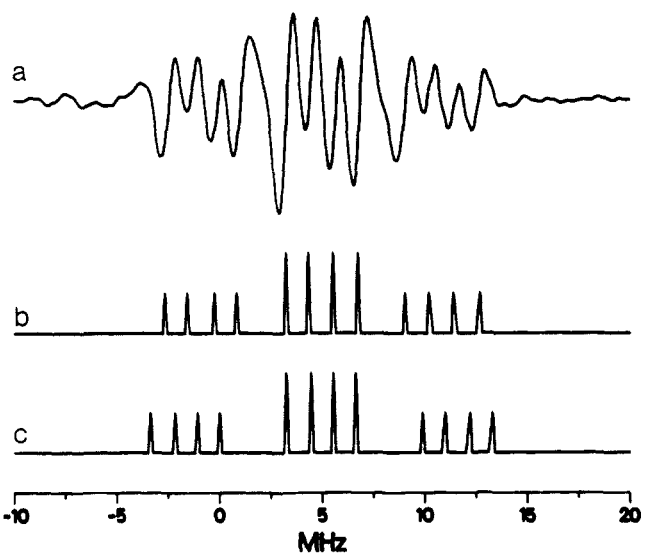

Figure 1. (a) FT-EPR spectra of the tetrad (T = 240 K) in dichloromethane. Microwave pulse is 44 ns after the laser pulse (591 nm, ~1 mJ/pulse). Positive going signals correspond to absorption and negative to emission. (b) Frequencies of the 12 hyperfine lines as determined from LP analysis. (c) Frequencies of the 12 hyperfine lines from the model quinone (see ref 17).

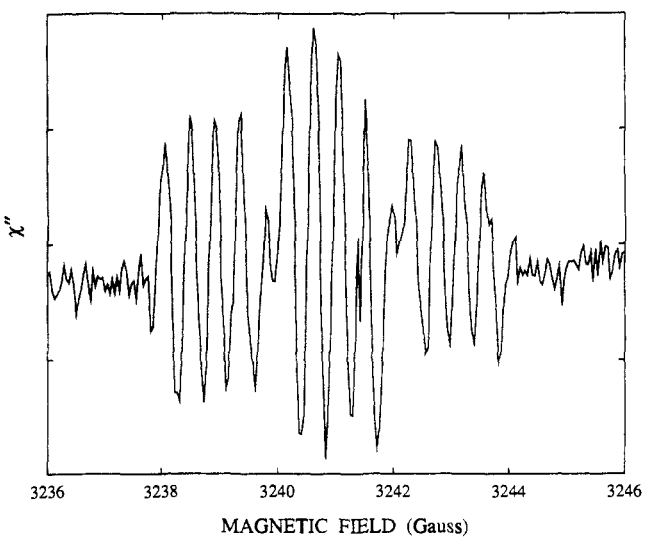

Figure 2. Diode-detected CW-EPR spectrum of the tetrad (T = 240 K) in dichloromethane. The spectrum was taken 1125 ns after laser excitation. Notice that the low and high field correspond to the high and low frequency, respectively, in the spectra in Figures 1a and 3.

duroquinone radical anions persisted for more than 6 months. This standard produces only a minor perturbation on the loaded Q of the strongly overcoupled resonator used in FT-EPR[6,7] and has been used successfully to set the phase and turning angle for samples with a broad range of dielectric properties ranging from large aqueous samples to polyacetylene, diamond, and quartz.

Spectra were analyzed by Fourier transform and linear prediction (LP)[14,15] techniques and by simulations in both the time and frequency domains. Diode detection CW-EPR experiments were carried out as described elsewhere,[16] using similar solutions of **1** in 3-mm o.d. Pyrex tubes at 240 K. The samples were photoexcited at 591 nm (25 mJ/pulse at 10 Hz) by a dye laser (Quanta Ray, PDL-1) pumped by the second harmonic of a Nd-YAG laser (Quanta Ray, DCR-1A).

Results and Discussion

EPR Spectra. The FT spectrum of the FID obtained with the microwave pulse 44 ns after the laser pulse is shown in Figure 1a. It appears to be a poorly resolved, first-derivative EPR spectrum containing 12 lines. No magnetic field modulation was used in these experiments, and the spectrometer was set to produce absorptive spectra, so this cannot be a first-derivative EPR spectrum. The appearance of the spectrum results from a combination of electron spin polarization and instrumental deadtime.[6] This deadtime produces wiggles adjacent to every line in the spectrum and, as is well-known in NMR spectroscopy, can obscure lines. In many cases, LP analysis is able to remove the deadtime effects and identify the true spectral lines. LP analysis identifies 12 major lines in the spectrum with frequencies that are consistent with hyperfine splitting of a single radical with couplings of 5.87 MHz (two protons), 2.38 MHz (one proton), and 1.15 MHz (one proton) with Lorentzian line widths of $1/(2\pi T_2)$ = 0.53 MHz and phases which are neither complete absorption nor emission. A stick spectrum based on the frequencies from the LP analysis is shown in Figure 1b and coincides with the 12 features in Figure 1a. This spectrum arises from the radical anion of Q_B, the 5.87-MHz hyperfine coupling comes from the two protons on the benzoquinone ring, while the two other couplings come from the magnetically inequivalent protons on the methylene bridge. This radical is similar to the radical anion of benzoquinone fused to a bicycloheptyl group[17] which has hyperfine couplings at analogous positions of 6.61, 2.24, and 1.12 MHz, respectively. A stick spectrum based on these couplings is shown in Figure 1c. Based on the similarities between stick spectra 1b and 1c, it is reasonable to conclude that the species generated from **1** establish (1) that it contains the radical anion of the Q_B moiety and, therefore, (2) that charge separation has indeed occurred. These conclusions are supported by the diode-detected CW-EPR spectrum depicted in Figure 2 which contains all 12 lines and shows the same derivative-like lines.[18] Thus, the derivative-like appearance of the spectra likely reflects strong electron spin polarization and not an experimental artifact. Establishing the exact polarization pattern is the key for determining the electron spin dynamics of

(14) Tang, J.; Norris, J. R. *J. Magn. Reson.* **1988**, *79*, 190.
(15) Tang, J.; Lin, C. P.; Bowman, M. K.; Norris, J. R. *J. Magn. Reson.* **1986**, *69*, 180.
(16) Gonen, O.; Levanon, H. *J. Phys. Chem.* **1985**, *89*, 1637.
(17) Kosman, D.; Stock, L. M. *J. Am. Chem. Soc.* **1969**, *91*, 2011.
(18) Diode-detection CW-EPR spectroscopy of transient radicals is also susceptible to line-shape distortions due to finite signal acquisition time. However, these distortions are different from those of FT-EPR (results from our laboratory).

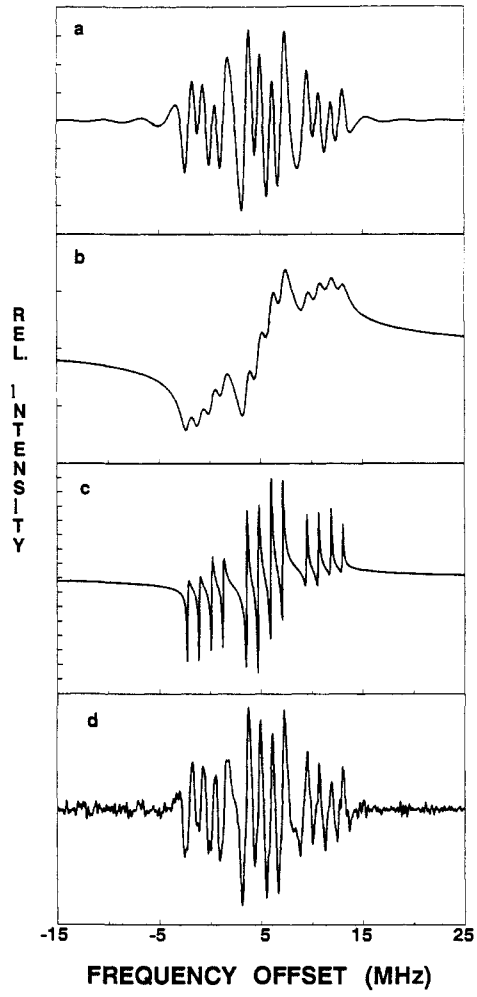

Figure 3. The real part of the Fourier transform of calculated and experimental FIDs. Positive going signals are absorptive and negative are emissive. The frequency scale denotes the difference between the EPR resonant frequency and the microwave carrier frequency so that lines at high frequency would appear at low magnetic field in a conventional EPR experiment (cf. Figure 2): (a) from the calculated FID with the initial points in the FID set to zero to duplicate the effect of the spectrometer's deadtime for comparison with Figure 1a; (b) from the entire best-fit calculated FID; (c) from the calculated FID multiplied by a decaying Gaussian and an increasing exponential function for resolution enhancement, showing the phase and intensity of each line; (d) from the experimental FID multiplied by a decaying Gaussian and an increasing exponential function for resolution enhancement (notice the similarity between this spectrum and that of Figure 2).

the charge separation reaction (see below).

FT-EPR Spectral Analysis and Electron Spin Polarization. The LP analysis produces tables of EPR frequencies, line intensities, and line phases. Although the electron spin polarization can be determined from this tabular output, examination of the predicted spectra can provide the same qualitative information in a more accessible form. An LP analysis utilizing the 12 hyperfine lines described above was made of the experimental FID. The resultant fit is the best description of the FID in terms of the Q_B radical anion. The portion of the best-fit FID at times longer than the instrumental deadtime (~120 ns) was processed in the same manner as the spectrum in Figure 1a to give the best-fit spectrum in Figure 3a. There is excellent agreement between the experimental and best-fit spectrum as well as for the FIDs. The agreement indicates that the experimental FID is describable as the Q_B radical anion with a Lorentzian line shape for each hyperfine line. Therefore, the unusual appearance of the spectrum must be caused by the electron spin polarization. The LP reconstruction of the experimental spectrum does not answer the questions concerning the electron spin polarization since the spectrum in Figure 3a contains the same deadtime distortions as the spectrum in Figure 1a. However, unlike the experimental data, values for the best-fit FID do exist for times less than the deadtime. The entire best-fit FID can be processed to give the spectrum in Figure 3b. This is the best estimate of the actual EPR spectrum of the sample based on the recorded portion of the FID. It clearly shows 12 hyperfine lines, although more poorly resolved than the original spectrum in Figure 1a. The instrumental deadtime has produced an artificial narrowing of the FT-EPR line widths in Figure 1a which has increased the apparent resolution but with a considerable amount of intensity loss. This is a well-known effect in experimental NMR spectroscopy. Figure 3b appears to contain 12 lines superimposed on a broad line centered at about 5 MHz. This is caused by overlap of the tails from the 12 Lorentzian lines of equal 0.53-MHz width. Electron spin polarization is apparent from Figure 3b; i.e., the low-frequency side of each component in the spectrum is more emissive and the high-frequency side more absorptive. However, the long Lorentzian tails from the different hyperfine lines makes it difficult to determine visually exactly what the intensity or polarization of each hyperfine line is. That information exists in the tables of amplitudes and phases of the individual lines obtained from the LP analysis. This can be visualized by constructing a spectrum with the proper amplitudes and phases but with sharper lines. Thus, the calculated FID was multiplied, before processing, by a filter consisting of a rising exponential and a falling Gaussian. Such a procedure, which is a common technique in NMR spectroscopy, narrows the spectral lines and makes them more Gaussian at the expense of increasing the noise level. The resulting spectrum is shown in Figure 3c. Each line is clearly resolved and shows an unusual low-frequency emission and high-frequency absorption. In addition, the relative line intensities are consistent with the assignment of the Q_B radical anion. The same manipulation, as was done to produce Figure 3c, was carried out on the experimental FID to produce the resultant spectrum in Figure 3d. It clearly shows three sets of four lines with relative intensities of roughly 1:2:1, and each of those 12 lines having low-frequency emission and high-frequency absorption. This spectrum is extremely important because (1) it supports the hyperfine assignment from the LP analysis far better than the spectrum in Figures 1a, 3a, or 3b; (2) the similarity between Figures 3c and 3d shows that the LP analysis has not produced any serious artifacts; (3) it is in full agreement with the diode-detected CW-EPR spectrum in Figure 2; (4) it is an independent confirmation of the electron spin polarization pattern that makes no assumptions about the line shape or composition of the EPR spectrum. Thus, Figure 3d is an independent validation of the LP analysis. This complementary spectral analysis clearly indicates that the spectrometer deadtime in the present experiments has produced no fundamental changes in the spectral line shape.

Origin of Spin Polarization. The FT- and CW-EPR spectra consist of the 12 hyperfine lines of the Q_B moiety, with each line being a mixture of absorption and emission. This strong ESP pattern can arise in two different ways. (1) The unresolved hyperfine splitting from the two remaining protons on the bicycloheptyl ring on Q_B may be strongly polarized in such a way that one side of each line is in emission and the other in absorption.[19] However, there is no obvious method for producing this sort of polarization. (2) There may be a residual electron spin–spin interaction between the Q_B radical anion and the carotenoid radical cation, producing an unresolved splitting of each line. ESP produced by a correlated-radical-pair type of mechanism would produce polarization in each of the hyperfine lines as observed.[20,21] Although both of these possibilities might give similar EPR spectra, they are distinguishable on the basis of the dependence of the FT-EPR signal intensity on the turning angle, θ_1, of the microwave pulse.

(19) Buckley, C. D.; Hunter, D. A.; Hore, P. J.; McLauchlan, K. A. *Chem. Phys. Lett.* **1987**, *135*, 307.
(20) Closs, G. L.; Forbes, M. D. E.; Norris, J. R. *J. Phys. Chem.* **1987**, *91*, 3592.
(21) Morris, A. L.; Thurnauer, M. C.; Tang, J. H.; Norris, J. R. *J. Chem. Phys.* **1990**, *92*, 4239.

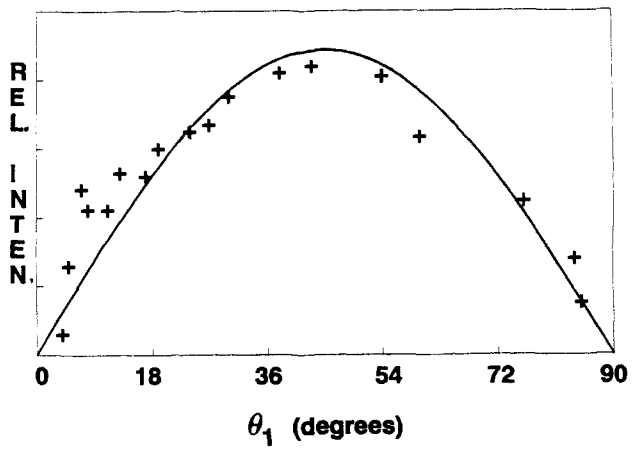

Figure 4. Dependence of the FT-EPR signal amplitude on the microwave pulse angle for the line nearest an offset frequency of zero. The turning angle was calibrated with stable duroquinone anion radical (90° pulse for the maximum intensity). The solid line is the fit of $A \sin(2\theta_1)$ to the experimental points.

For case 1, the intensity of the FT-EPR spectrum is proportional to $\sin(\theta_1)$ with a maximum when $\theta_1 = \pi/2$, as is true of any unpolarized, stable free radical, e.g., duroquinone radical anion. On the other hand, case 2 involves interacting electron spins where the ESP depends on the spin state of both electron spins in the radical pair. In this case, if both electron spins are excited by the microwave pulse, the ESP is destroyed because the electron spin states are essentially scrambled by the pulse, and the FID disappears. The spectrum intensity is proportional to $\sin(2\theta_1)$ and is maximum when $\theta_1 = \pi/4$ or 45°. A similar situation occurs in the study of chemically induced dynamic nuclear polarization (CIDNP) by FT-NMR, where homonuclear couplings can produce analogous effects.[22]

We therefore examined the turning angle dependence of the FT-EPR spectrum from the tetrad. The signal intensity fits the $\sin(2\theta_1)$ profile predicted for case 2 and has a maximum at approximately $\theta_1 = \pi/4$ (cf. Figure 4). This is precisely as expected for a polarized, interacting radical pair. This provides conclusive proof that the tetrad, upon light excitation, produces a long-lived interacting radical pair state although only the Q_B radical anion is observed in the one-pulse experiment. Both the observation of the ESP and the recombination of the separated charges depend on the electron spin–spin interaction between the Q_B radical anion and the carotenoid radical cation moieties. The interaction must be small because the lifetime of the charge-separated species is rather long and because the spin–spin splitting is not resolved in the EPR spectrum. The coupling is certainly less than the smallest resolved hyperfine coupling of 1.15 MHz in the Q_B radical anion, or the 0.53-MHz line width.

Carotenoid Cation Radical. The carotenoid radical cation should not be observed in the one-pulse FT-EPR experiments because of its large line width. Grant et al.[23] have reported an EPR line width of 1.36 mT, or 38.1 MHz, for the radical cation of β-carotene in dichloromethane. The FID from a radical with such a spectrum decays in about 5 ns and would be lost in the deadtime of the spectrometer. However, the line width of the carotenoid radical cation is produced by large, inhomogeneous broadening from the proton hyperfine interaction and can be refocused in a two-pulse spin–echo experiment. Therefore, the shape of the electron spin–echo was recorded in a two-pulse experiment. The echo was Fourier transformed to produce the spectrum in Figure 5. The spectrum shows not only the Q_B radical anion spectrum present in the FID, but also another broad response at lower frequencies (smaller g-factor) than the Q_B radical anion which decays at the same rate after the laser as the Q_B radical anion.

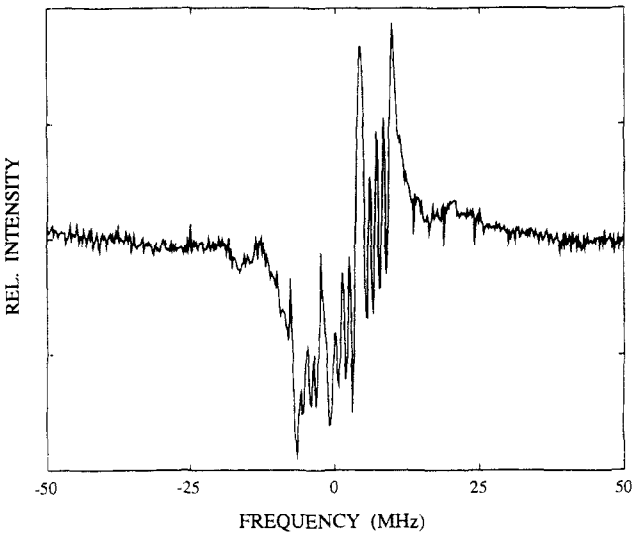

Figure 5. Two-pulse FT-EPR spectrum of the tetrad. This spectrum is the FT of the echo formed by two microwave pulses, 44 ns after the laser pulse. The carotenoid radical cation is the broad emissive signal on the lower frequency half. The Q_B radical anion is superimposed on the cation signal. It should be noted that both signals disappear with the same rate.

Its kinetics show it to be the geminate partner of the radical anion which optical spectroscopy places on the carotenoid moiety.[11-13] The response is much narrower than expected for the unpolarized carotenoid radical cation but is consistent with a polarized carotenoid radical. The bandwidth of the two-pulse spin–echo experiment is much less than that of the FID, and consequently some intensity in the wings of the carotenoid spectrum is lost. Only a portion of the emissive part of the spectrum is observable in this figure, and it is not suitable for determining either the g-factor, the line width, or the expected emission/absorption line shape of the carotenoid cation radical. Nevertheless, we have succeeded in simultaneously observing both radical ion species in this interacting radical pair. It should be noted that all attempts to detect the carotenoid radical cation using CW-EPR detection failed. This may be partially due to the nearly 70-fold difference in line widths and comparable diferences in amplitude between the Q_B radical ion (0.53 MHz) and the carotenoid radical cation (38.1 MHz). A similar situation occurs in the CW-EPR detection of electron transfer from triplet porphyrins to quinones where only the quinone radical anion is detected and the identification of the porphyrin radical cation is ambiguous owing to inhomogeneous broadening.[24] On the other hand, upon deuteration of the porphyrin moiety the porphyrin radical cation has its spectrum sharpened.[25] It is perhaps more remarkable that the carotenoid is observed at all in Figure 5, but that may be due to differences in the relaxation times, T_2, of the anion and cation.

Kinetics. The kinetics of the formation and decay of the charge-separated radical pair species was measured from the FT-EPR spectra by varying the time delay between the laser pulse and the microwave pulse. The intensity of the Q_B radical anion is shown as a function of this delay, in Figure 6. The solid line is a least-squares fit to a kinetic model with unimolecular production and decay of radical pair via radical-pair mechanism (RPM) with no contribution of a triplet mechanism:[26]

$$P_{RPM} = A[\exp(-t/\tau) - \exp(-kt)] \quad (1)$$

where A is the signal amplitude, τ is a combination of spin–lattice relaxation (SLR) time of the Q_B radical and the charge recom-

(22) Schäublin, S.; Höhener, A.; Ernst, R. R. *J. Magn. Reson.* **1974**, *13*, 196.
(23) Grant, J. L.; Krammer, V. J.; Ding, R. S.; Kispert, L. D. *J. Am. Chem. Soc.* **1988**, *110*, 2151.
(24) Results from our laboratory and ref 25. However, one report of an unambiguous identification, by CW-EPR detection, of the porphyrin (undeuterated) cation in a well-studied porphyrin–quinone system is: Möbius, K.; Lubitz, W.; Plato, M. In *Advanced EPR*; Hoff, A. J., Ed.; Elsevier: Amsterdam, 1989; Chapter 13.
(25) van Willigen, H.; Voulle, M.; Dinse, K. P. *J. Phys. Chem.* **1989**, *93*, 2441–2444.
(26) It was impossible to fit the experimental data points in Figure 6 when triplet mechanism terms were included in eq 1.

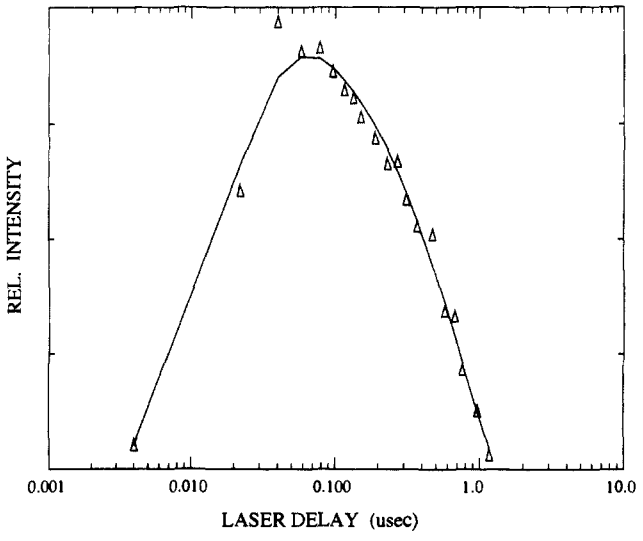

Figure 6. Signal intensity of the Q_B radical anion as a function of the laser delay. The superimposed solid line is the result of best fit analysis as described by eq 1.

bination (back reaction) time, and k is a combination of the spectrometer response and the electron-transfer rate (see also ref 9). The rise time of the signal is 16 ns, which is determined by the width of the laser and microwave pulses and can only provide an upper limit for the time of the production of the final radical pair state. The signal decays with a time constant of 500 ns (240 K), somewhat faster than the decay of the carotenoid radical cation at this temperature as detected optically. The enhanced decay rate of the EPR signal could be due to the contribution of SLR and/or to the influence of the magnetic field on the charge recombination reaction. The shape of the spectrum does not change as the laser delay is increased.

Reaction Route (Spin Multiplicity). An important question concerning this light-driven charge separation is whether the reaction proceeds from a singlet state, as in natural photosynthesis, or from the triplet state. This can be answered by a careful consideration of the ESP in the charge-separated, radical pair species (assuming $J < 0$). The ESP polarization is low-frequency (high magnetic field) emission and high-frequency (low magnetic field) absorption which obeys the sign rules for spin polarization in interacting radical pairs[20,21] for singlet-state reactions but not for triplet reactions. Also, both the experimental and the fitted spectra show that the spectrum of the Q_B radical anion is nearly antisymmetric with respect to the center of its spectrum. This means that there are equal amounts of absorption and emission in the spectrum. Thus, there is no net ESP to within the experimental noise and consequently no net spin angular momentum in the charge-separated radical pair. The absence of net spin angular momentum suggests a reaction from the singlet state, which also has no net spin angular momentum. This conclusion is consistent with fluorescence quenching experiments which indicated an excited-state lifetime of 15 ps for the precursor to the radical pair which is too fast for involvement of a triplet state. Thus, the evidence is strong that the tetrad undergoes singlet photochemical reactions to produce a relatively long-lived, charge-separated radical pair species.

In summary, we have demonstrated that fast CW- and pulsed-EPR spectroscopies can be used to monitor singlet photochemistry and complement optical spectroscopy. More importantly, they have identified the long-lived, photoinduced state of **1** to be a charge-separated radical-ion pair generated by electron transfer from the excited singlet state.

Acknowledgment. This work was supported by the Division of Chemical Sciences, Office of Basic Energy Sciences, Office of Energy Research, U.S. Department of Energy [(Contract W-31-109-Eng-38, (J.R.N.), and Grant DE-FG02-87 ER13791 (D.G. and T.A.M.))] and by U.S.-Israel BSF Grant 86-00020 (H.L.). The Fritz Haber Research Center is supported by the Minerva Gesellschaft für die Forschung, GmbH, München, FRG. This is publication No. 53 from the Arizona State University Center for the Study of Early Events in Photosynthesis. The Center is funded by the U.S. Department of Energy (Grant No. DE-FG02-88ER13969) as part of the USDA/DOE/NSF Plant Science Center program. This work is in partial fulfillment of the requirements for the accomplishment of an M.Sc. degree (K.H.) at the Hebrew University of Jerusalem. We thank Dr. M.C. Thurnauer for helpful discussions.

Registry No. 1, 112296-44-3.